MOLECULAR ONCOLOGY 1 (2007) 216–225

available at www.sciencedirect.com

www.elsevier.com/locate/molonc

Low-volume, high-throughput sandwich immunoassays for profiling plasma proteins in mice: Identification of early-stage systemic inflammation in a mouse model of intestinal cancer

Sara Forrester[a], *Kenneth E. Hung*[b], *Rork Kuick*[c], *Raju Kucherlapati*[b], *Brian B. Haab*[a,*]

[a]*Van Andel Research Institute, 333 Bostwick, Grand Rapids, MI 49503, USA*
[b]*Partners Healthcare Center for Genetics and Genomics, Harvard Medical School, Boston, MA 02115, USA*
[c]*University of Michigan Cancer Center Biostatistics Cores, University of Michigan, Ann Arbor, MI 48109, USA*

ARTICLE INFO

Article history:
Received 10 April 2007
Received in revised form
1 June 2007
Accepted 1 June 2007
Available online 15 June 2007

Keywords:
Proteomics
Plasma protein profiling
Low-volume sandwich-immunoassays
Mouse cancer model

ABSTRACT

Mouse models of human cancers may provide a valuable resource for the discovery of cancer biomarkers. We have developed a practical strategy for profiling specific proteins in mouse plasma using low-volume sandwich-immunoassays. We used this method to profile the levels of 14 different cytokines, acute-phase reactants, and other cancer markers in plasma from mouse models of intestinal tumors and their wild-type littermates, using as little as 1.5 μl of diluted plasma per assay. Many of the proteins were significantly and consistently up-regulated in the mutant mice. The mutant mice could be distinguished nearly perfectly from the wild-type mice based on the combined levels of as few as three markers. Many of the proteins were up-regulated even in the mutant mice with few or no tumors, suggesting the presence of a systemic host response at an early stage of cancer development. These results have implications for the study of host responses in mouse models of cancers and demonstrate the value of a new low-volume, high-throughput sandwich-immunoassay method for sensitively profiling protein levels in cancer.

1. Introduction

Proteomics technologies hold great potential for the discovery of cancer biomarkers (Etzioni et al., 2003). While proteomics technologies have significantly and steadily advanced in recent years, the identification of low-abundance cancer markers amidst complex backgrounds of high-abundance and highly variable proteins has been difficult. An approach to overcoming the problem of variability between specimens and conditions is to use animal models of cancer (Kuick et al., 2007; Shaw et al., 2005). Genetic backgrounds and environmental and sample collection conditions can be precisely controlled in animal models, which reduces the normal variability between subjects and permits easier identification of cancer-related protein alterations. Mass-spectrometry-based studies of the proteomes of mouse models of cancer are currently underway.

Antibody-based methods are a useful complement to mass-spectrometry- and separations-based technologies. For proteomics studies in mouse models of cancer, the ability to analyze multiple proteins using low sample volumes would be particularly useful. Many groups have demonstrated the use of antibody microarrays as a means to multiplex the detection of specific proteins (see reviews in Haab, 2006; Kingsmore, 2006; Wingren and Borrebaeck, 2006). Although significant progress in these technologies has been made,

* *Corresponding author*. Tel.: +1 616 234 5268; fax: +1 616 234 5269.
E-mail address: brian.haab@vai.org (B.B. Haab).
1574-7891/$ – see front matter © 2007 Federation of European Biochemical Societies. Published by Elsevier B.V. All rights reserved.
doi:10.1016/j.molonc.2007.06.001

a practical strategy for routine application to mouse proteomics studies has yet to be established.

One approach to multiplexing antibody assays is to directly label all the proteins in a sample with a tag (such as biotin or Cy3) and detect the level of tag bound at each antibody after incubation of the sample on an antibody array (Haab et al., 2001; Sreekumar et al., 2001; Wingren et al., 2005). This method is simple and efficient for broad screening and discovery, but is not as effective for the quantitative and highly-specific detection of a set of candidate markers. Sandwich assays provide highly sensitive and specific detection and have been multiplexed on microarrays (Huang et al., 2001; Schweitzer et al., 2002; Li and Reichert, 2003; Geierstanger et al., 2006). In this approach, the amount of protein bound to each capture antibody on an array is probed with a labeled detection antibody, and multiple, different detection antibodies are mixed into one solution. A limitation of this approach is the difficulty in identifying matched capture and detection antibody pairs that demonstrate no cross reactivity between proteins or antibodies. Systematic routines have been worked out for screening for cross-reactivity among a set of purified proteins (Perlee et al., 2004), but such tests do not rule out the possibility of cross-reactivity in certain biological samples due to the occasional presence of large protein complexes. Also, optimal sample dilution factors might not be equivalent between certain analytes, making their multiplexed detection in a single assay difficult. Sandwich assays also have been multiplexed using bead-based assays (Vignali, 2000), which have similar constraints and added concerns over potential interactions between different capture antibodies in the same mixture.

One goal of this work was to develop an antibody-based tool that is well-suited to the rapid and routine measurement of specific protein levels in mouse models of cancers. Rather than multiplexing sandwich assays in a single assay, we detect single analytes in each assay, and use low-volume, high-throughput methods so that many individual assays can be run. In this way, the total sample volume consumed is similar to the multiplexed approach, and the time per assay can be made similar, while eliminating the possibility of cross-reactivity and reducing the time of developing and validating the multiplexing. This approach was made possible by the development of a versatile and practical method to process multiple arrays of varying sizes on each microscope slide.

A second goal of this work was to apply this method to measuring multiple, specific proteins in the plasma of a mouse model of human cancer. We used a murine intestinal tumor model which carries a single-codon mutation in the Adenomatous Polyposis Coli (APC) gene and reliably develops 30–40 intestinal adenomas by 4 months of age (Su et al., 1992). The APC gene has been established to be the most important initial mutation for entry into the adenoma-carcinoma pathway, and germline mutation in the human APC gene results in the CRC predisposition syndrome Familial Adenomatous Polyposis (FAP) (Kinzler and Vogelstein, 1996). Previous proteomics profiling of plasma from this model showed significant protein elevations relative to the wildtype counterpart mice (Hung et al., 2006). As initial targets for the antibody arrays, we chose proteins that could have altered levels in the plasma after the onset of intestinal cancer, including inflammatory cytokines, acute-phase reactants, and the mucin MUC1. These proteins allowed us to test the ability of our system to detect changes in protein expression in mouse plasma and to profile the extent of a systemic host response in this mouse model, which may be useful for later studies on those systems. Also, we chose both high-abundance and low-abundance proteins to test the performance of the method for a wide range of targets.

2. Results

2.1. *Development of low-volume, high-throughput sandwich assays*

In order to efficiently process many low-volume antibody arrays, we used a custom-made device to imprint wax patterns onto the surfaces of microscope slides, creating hydrophobic partitions that segregate various samples (Figure 1a). Distinct stamp designs can be used to form differing sizes and numbers of partitions on each slide. For this study, we used a design that partitions 48 arrays on each slide, with each array composed of up to 144 distinct spots, and another design that partitions 192 arrays on each slide, with each array containing up to 12 spots. The larger array requires 6 μl of sample per array, and the smaller requires 1.5 μl of sample per array. The spacing of the arrays has been made compatible with standard multi-channel pipettes for eventual automation.

Such a design enables the efficient processing of many samples or conditions in parallel, using small volumes per assay. For the experiments described below, we used eight of the arrays on each slide for calibration standards with known concentrations of a particular analyte, and we used the rest of the arrays for samples (Figure 1b). A single detection antibody then detected the level of an analyte on each slide. Since we spotted multiple capture antibodies but used only a single detection antibody on each array, only the capture antibody corresponding to the detection antibody was used to measure the level of the analyte, and the other antibodies served as negative controls (Figure 1c).

Pairs of capture and detection antibodies were tested for each target using serial dilutions of antigens (Figure 2). We used dilutions of purified antigen if the antigen was commercially available (11 targets), and we used dilutions of pooled mouse plasma if not (9 targets). In ten cases, two different antibodies were available as the capture and detection antibodies, but for the other cases, only one antibody was available, and that antibody was used both as capture and detection (Table 1). Of the 20 sandwich assays for which we attempted development, 14 produced sigmoidal binding curves that indicated proper antibody–antigen interactions (representative curves shown in Figure 2). For three of the attempted assays we used antibodies that were raised against human antigens, to test whether the cross-reactivity to the mouse sequence would be sufficient to achieve antigen binding in pooled plasma. None of those assays showed signal. The other three failed assays used antibodies that were raised against mouse sequences but showed flat binding curves. A summary of the attempted assays and results is provided in Table 2.

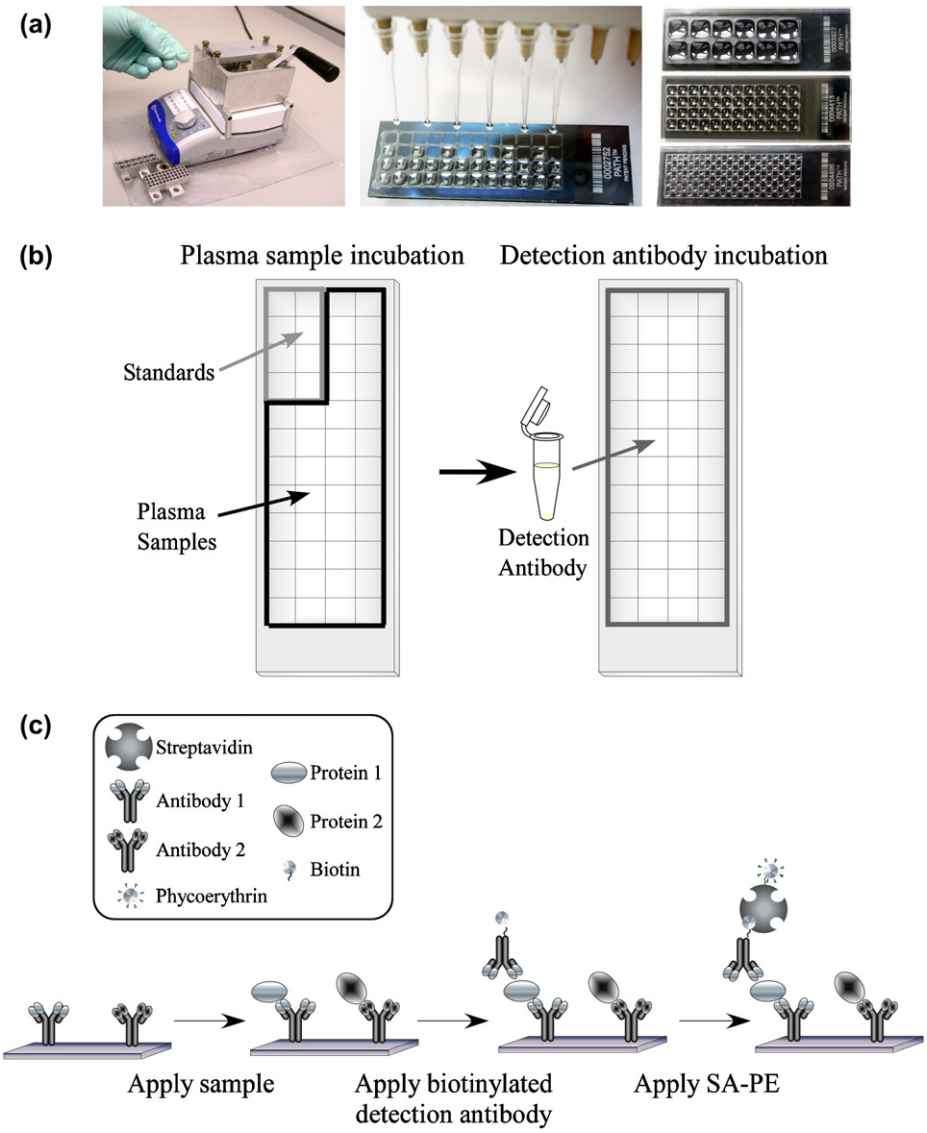

Figure 1 – An approach to high-throughput sample processing. (a) Wax is imprinted onto a microscope slide to form borders around multiple arrays. Wax is melted by the hotplate under the bath, and a slide is inserted upside-down into the holder. Bringing the lever forward raises a stamp out of the wax bath to touch the slide, imprinting the design onto the slide. Two stamps are shown in front of the device (left image). The arrays are spaced by 4.5 mm, which is compatible with the 9 mm spacing of standard multi-channel pipettes (middle). Samples loaded onto slides containing 12, 48, and 192 (96 samples loaded) arrays per slide are shown (right image). (b) A plan for incubating 40 different samples and eight standards on one slide, with detection by a single detection antibody. (c) Schematic illustration of a sandwich assay with fluorescence detection. Two different antibodies on an array are illustrated, and the detection antibody binds only its targeted protein bound by the corresponding capture antibody.

The detection limits determined from the dilution curves that used purified antigens ranged from 50 pg/ml to low pg/ml (Table 2 and Figure 2). These detection limits are similar to those achieved for sandwich enzyme-linked immunosorbent assays (ELISA) and should be sufficient to detect most cytokines, especially when elevated. The curves using dilutions of serum can be used to set a proper dilution factor for the individual samples. The dilution factor should be set so that most individual measurements fall in the linear range of the binding curve. For proteins with high endogenous concentrations like haptoglobin and hemopexin, we determined dilution factors of 10,000 and 100,000, respectively, but for mid-range proteins like CRP and plasminogen, we used dilution factors of 200 and 1000, respectively. We used a dilution factor of 2 for all the cytokines.

2.2. *Profiling protein levels in mutant and wildtype mice*

We next determined the levels of the 14 proteins in individual plasma samples from a cohort of mutant ($n = 39$) and wildtype ($n = 25$) mice. Two types of mutant mice were used, one with a nonsense mutation at codon 850 of the APC gene (APC^{Min}, $n = 15$), and the other with a nonsense mutation at codon 580 of the APC gene (APC Δ580, $n = 24$). We ran the samples

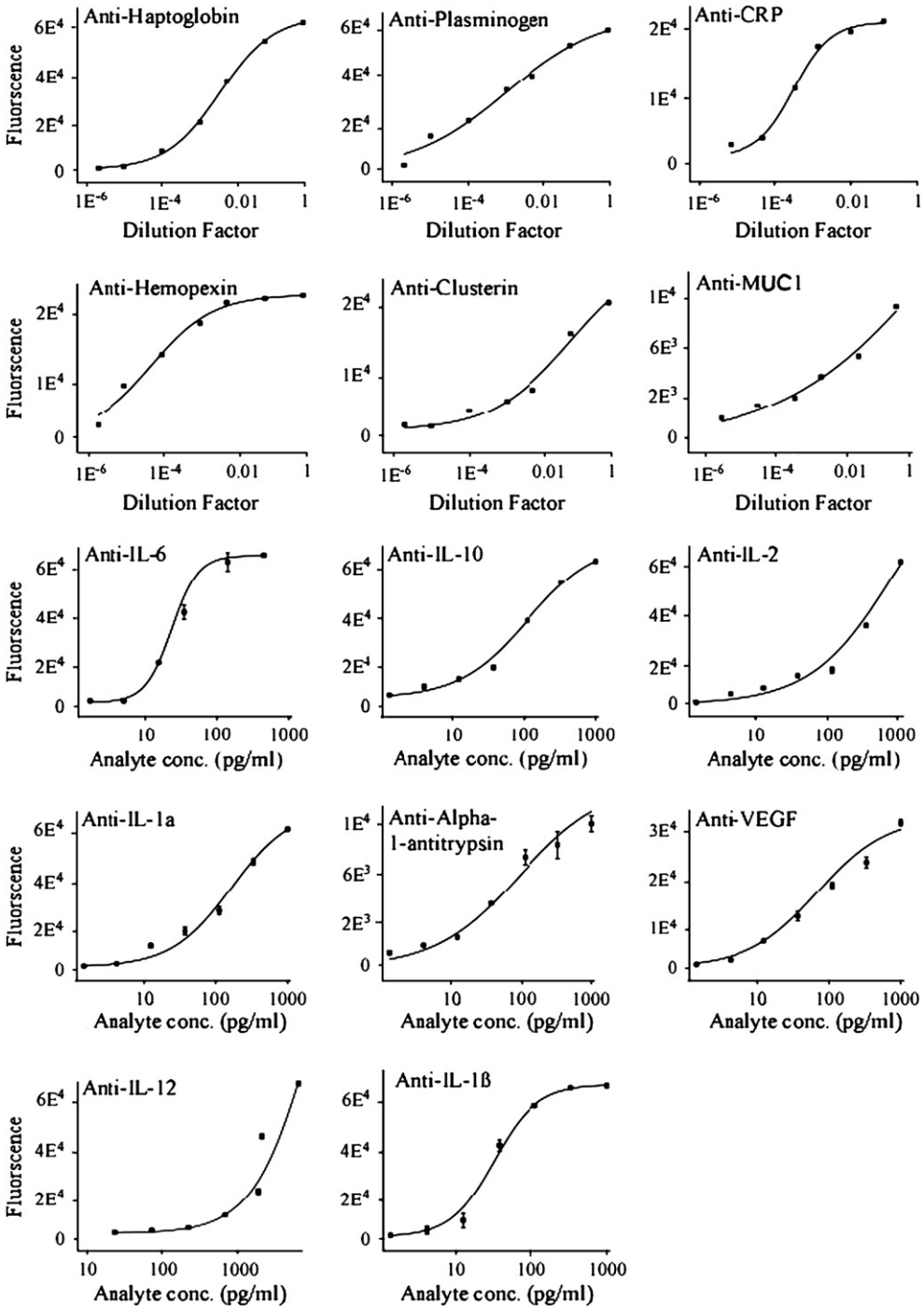

Figure 2 – Standard curves of selected microarray analytes. Calibration curves were created by plotting the raw fluorescence signal (arbitrary units) against the concentration of purified antigens (pg/ml) or against the dilution factor of pooled mouse plasma sample. The zero-concentration data point is not included because of the log-scale on the *x*-axis.

in a different, randomized order on the microscope slides with each assay, along with a dilution curve of either purified antigen or pooled plasma. The dilution curve provided a means to convert the raw fluorescence values to concentration (if dilutions of purified antigen were used) or to concentration units (if dilutions of pooled plasma were used). We used the 48-array format for seven of the assays and the 192-array format for ten, with both formats for three.

We investigated the agreement between the larger array format, using 6 μl per array, and the smaller array format, using just 1.5 μl per array, for measurements of the protein IL-12 with arrays that were printed and run in the same batch. The results showed a significant correlation over all the samples ($r = 0.85$) between the two formats (Figure 3b), indicating a general correspondence in the assays. The correlation between the standard curves was very high ($r = 0.99$, data not

Table 1 – The antibodies and proteins used

	Capture/detection	Source	Catalog number
Antibody			
Anti-human sialyl Lewis A	Both	Abcam	ab3982
Anti-human tenascin C	Both	R & D Systems	Mab2138
Anti-human von Willebrand factor	Both	DAKO	A0082
Anti-mouse alpha 1 antitrypsin	Both	Abcam	Ab14226
Anti-mouse clusterin	Both	R & D Systems	AF2747
Anti-mouse CRP	Both	R & D Systems	AF1829
Anti-mouse cytochrome c	Capture	BD Pharmingen	556432
Anti-mouse cytochrome c-biotinylated	Detection	BD Pharmingen	556432
Anti-mouse haptoglobin	Both	Life Diagnostics	18141
Anti-mouse hemopexin	Both	Immunology Consultants Laboratory	CHX90A
Anti-mouse IL-10	Capture	BD Pharmingen	551215
Anti-mouse IL-10-biotinylated	Detection	BD Pharmingen	554465
Anti-mouse IL-12	Capture	BD Pharmingen	551219
Anti-mouse IL-12-biotinylated	Detection	BD Pharmingen	554476
Anti-mouse IL-1a	Capture	BD Pharmingen	550604
Anti-mouse IL-1a-biotinylated	Detection	BD Pharmingen	550606
Anti-mouse IL-1b	Capture	BD Pharmingen	550605
Anti-mouse IL-1b-biotinylated	Detection	R & D Systems	BAF401
Anti-mouse IL-2	Capture	BD Pharmingen	554424
Anti-mouse IL-2-biotinylated	Detection	BD Pharmingen	554426
Anti-mouse IL-6	Capture	BD Pharmingen	554400
Anti-mouse IL-6 -biotinylated	Detection	BD Pharmingen	554402
Anti-mouse MCP-1	Capture	BD Pharmingen	551217
Anti-mouse MCP-1-biotinylated	Detection	BD Pharmingen	554444
Anti-mouse MUC-1	Both	Genway	A22681
Anti-mouse plasminogen	Both	Oxford Biomedical Research	PL64
Anti-mouse troponin C	Both	Biodesign	H86742
Anti-mouse VEGF	Capture	R & D Systems	AF493NA
Anti-mouse VEGF-biotinylated	Detection	R & D Systems	BAF493
Protein			
Alpha-1-antitrypsin	Recombinant protein	Research Diagnostics	AB14226
Cytochrome c	Recombinant protein	R & D Systems	709cc
IL-10	Recombinant protein	BD Pharmingen	550070
IL-12	Recombinant protein	R & D Systems	419ML
IL-1a	Recombinant protein	R & D Systems	400ML
IL-1b	Recombinant protein	BD Pharmingen	554577
IL-2	Recombinant protein	R & D Systems	402ML
IL-6	Recombinant protein	BD Pharmingen	554582
MCP-1	Recombinant protein	BD Pharmingen	554590
Troponin C	Recombinant protein	Biodesign	A86562M
VEGF	Recombinant protein	Biodesign	A52532M

shown), probably due to the lack of a complex background and indicating that antibody spotting or binding is not the main source of variability between assays. The intra-assay variability was slightly higher for the smaller format, with a median coefficient of variation (CV) between replicate antibody spots of 11% for the smaller array versus 9% for the larger array. The median CV between the formats was 18%, reflecting the contributions of the separate sources of variability.

The mutant mice had higher levels of most of these proteins than the wildtype mice, with very high statistical significance (Figure 3a). The most consistently elevated protein was CRP, which was elevated in cancer with a 90% sensitivity at an 80% specificity. An elevation in haptoglobin, hemopexin, and plasminogen in this mouse model (using different samples) was previously seen using mass spectrometry methods (Hung et al., 2006).

The mice had variable numbers of tumors in the intestinal tract at the time of sample collection, and the number of tumors generally increased with the age of the mice. We correlated the concentrations of the proteins with the number of tumors and age of the mice to investigate the relationship between those parameters (Table 3). In the mutant mice, only IL-6, IL-12, haptoglobin, and hemopexin showed significant correlations with age or number of tumors. None of those proteins showed correlation with age in the wildtype mice, indicating that the elevations in these proteins was not related to the age of the mice but rather to the presence of the tumors. No proteins showed statistically significant differences between the APC^{Min} and APC Δ580 mice. The values from MUC1 and IL-1beta were removed because a high percentage of the samples gave a fluorescence signal below that of the lowest standard.

A view of the patterns of protein level ordered by number of tumors shows that for IL-6, haptoglobin, and hemopexin, the elevations mainly occur at a high tumor burden, above about 30–40 tumors (Figure 4). Some proteins are highly

Table 2 – Summary of assay development: the detection limits were determined from the dilution curves of Figure 2

	Standard curve	Dilution factor	Detection limit (pg/ml)
Sandwich assays developed			
Anti-mouse haptoglobin	Pooled plasma	1:1000	NA
Anti-mouse hemopexin	Pooled plasma	1:100000	NA
Anti-mouse plasminogen	Pooled plasma	1:1000	NA
Anti-mouse CRP	Pooled plasma	1:200	NA
Anti-mouse VEGF	Recombinant protein	1:2	1
Anti-mouse IL-12	Recombinant protein	1:2	30
Anti-mouse MUC-1	Pooled plasma	1:2	NA
Anti-mouse IL-10	Recombinant protein	1:2	1
Anti-mouse IL-6	Recombinant protein	1:2	1
Anti-mouse IL-2	Recombinant protein	1:2	4
Anti-mouse IL-1α	Recombinant protein	1:2	4
Anti-mouse IL-1β	Recombinant protein	1:2	4
Anti-mouse alpha-1 -antitrypsin	Recombinant protein	1:20	10
Anti-mouse clusterin	Pooled plasma	1:20	NA
Sandwich sssays unsuccessful			
Anti-human sialyl Lewis A	Pooled plasma		
Anti-human tenascin C	Pooled plasma		
Anti-human von Willebrand factor	Pooled plasma		
Anti-mouse troponin C	Recombinant protein		
Anti-mouse MCP-1	Recombinant protein		
Anti-mouse cytochrome *c*	Recombinant protein		

variable within the mutant mice, such as VEGF and alpha-1-antitrypsin, and others are more consistently elevated, such as CRP and IL-12. The protein levels are not highly correlated with each other, but most seem to show occasional elevations even in the mice with few tumors. Some proteins showed occasional elevations in the wildtypes, including alpha-1-antityrpsin and IL-1alpha.

Many have proposed using the combined expression of several markers to achieve improved diagnostic classification relative to single markers. Many algorithms are available for sample classification using panels of markers. Here we used diagonal linear discriminant analysis (DLDA) (Dudoit et al., 2002) to assign a score that can be used to classify the mice as either mutant or wildtype in leave-one-out cross validation. Panels of five or more of the protein measurements perfectly separated the samples ($p = 2 \times 10^{-18}$, rank-sum test, Figure 5a), as did using just three assays, and classifiers using two or four assays performed near-perfectly (Supplementary Figure 1). Surprisingly, the DLDA score was not significantly correlated ($p = 0.20$) with the number of tumors in the mice (Figure 5b), meaning that the classification of the young mice with low tumor burden was at most only slightly more difficult than the classification of the older mice with higher tumor burden.

We investigated the importance of each antibody in the classification by considering the absolute values of the scores from each antibody when using all 12 of them, and calculating what fraction of the sums of the absolute values of the scores for each sample was due to each antibody, on average. The top three were CRP, haptoglobin, and IL-12, contributing 17%, 14% and 14% of this sum on average, respectively. By the seventh best discriminating antibody (IL-10) this average had decreased to 8%, while the 11th best antibody (IL-6) contributed only 3%, and IL-1alpha, which did not show a significant difference between mutant and wild-type mice, contributed less than 1% to the sum on average (summarized in Supplementary Figure 2). Therefore no single marker is overwhelmingly influential in the classification, but the proteins with the highest individual significance play the biggest roles.

3. Discussion

The development of efficient methods to develop and run multiple sandwich immunoassays with low sample consumption is critical for the discovery and validation of biomarkers. Our strategy was different from that of previous efforts, which multiplexed the detection of multiple analytes using cocktails of detection antibodies. Instead, we used only one detection antibody per array and reduced the size and volume of each array. Since the volume of each assay was low, we could run multiple assays without a large amount of total sample consumption, and high-throughput processing makes the measurement of many analytes practical. This strategy makes assay development much quicker than for multiplexed assays and removes the possibility of cross-reactivity between assays.

Others types of low-volume immunoassays have appeared, such as a microfluidics system that flows liquid by centrifugal force in a spinning disk (Lai et al., 2004; Honda et al., 2005). Although studies analyzing sets of real samples have not appeared on those platforms, in principle a similar approach of running many low-volume, single-plex assays could be applied. However, the microfluidics platforms require significant expertise and specialized laboratories. The method described here uses equipment that is broadly available and could be readily adopted by many laboratories.

We demonstrated two sizes of arrays with proportionally varying numbers of spots, required sample volumes, and numbers of arrays per slide. Larger arrays might be better for assay development or initial screening, in which measurements of binding to a large number of antibodies in a limited number of samples are desired, and smaller arrays could be preferable for high-throughput measurements on a smaller number of antibodies. The intra-assay CVs of around 10% and inter-assay CVs of less than 20% are sufficient for research applications and similar to many other types of antibody assays. The CVs could be further reduced with additional

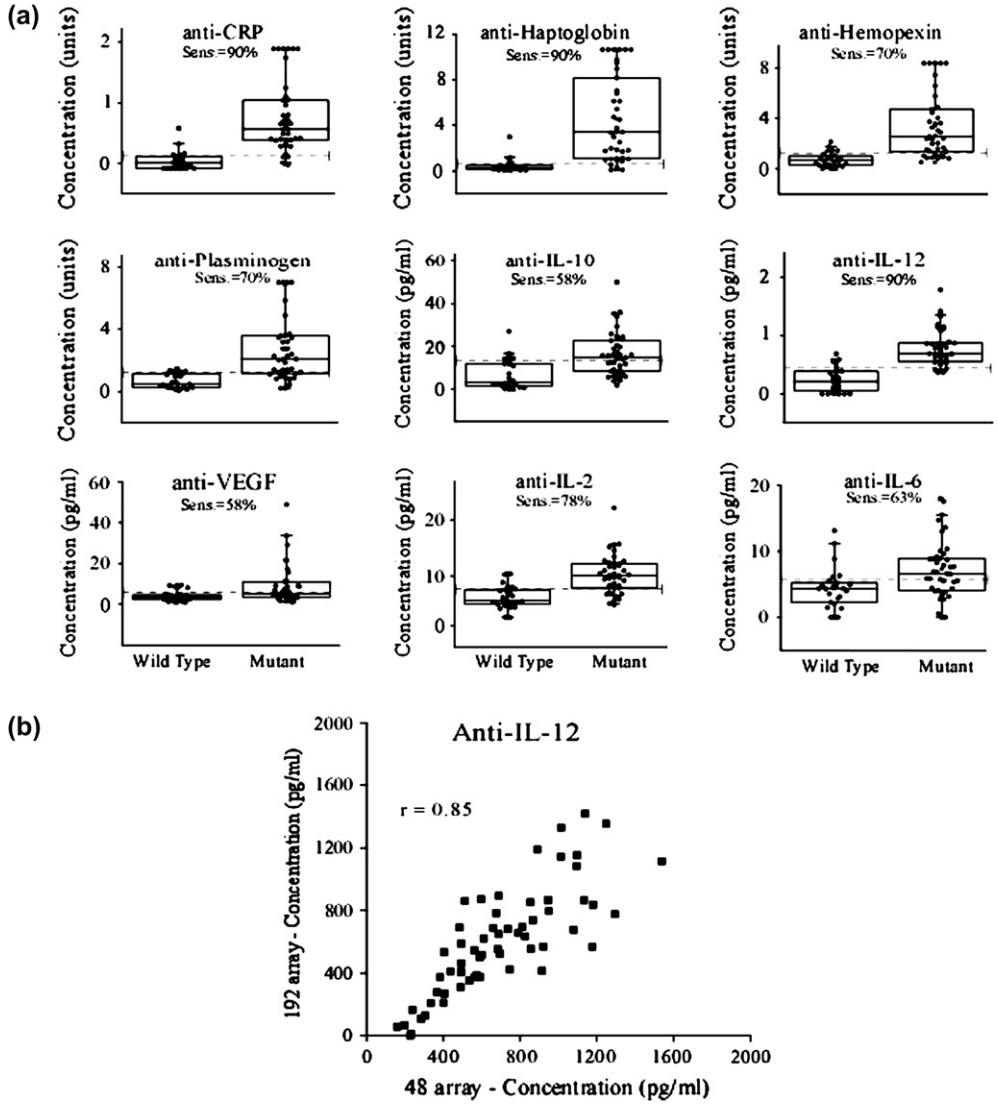

Figure 3 – Comparisons of levels in mutant and wildtype mice for selected analytes. (a) Distributions of concentrations. The concentrations of the indicated analytes for individual samples are indicated by each point, and the box in each plot defines the upper and lower quartiles of the distributions, with the line in each box indicating the median value. The dashed line in each plot represents the 80% specificity level (5/25 wildtype samples above the threshold), and the sensitivity at that threshold is given in each plot. (b) Scatter plot comparison of results obtained on larger arrays (48 arrays/slide) and smaller arrays (192 arrays/slide). The same set of samples was processed in parallel on two microscope slides printed with the two different array formats.

optimization and automation, which may enable diagnostic-grade applications.

The profiling of the cytokine and acute-phase-reactant levels revealed a strong systemic inflammatory response in the mutant mice. That response appears to occur even in the mice with very low tumor burdens, since the DLDA-based discrimination performed nearly as well on mice with few tumors as on those with many tumors, and since only a few of the individual proteins were positively correlated to tumor burden. These observations may indicate that a host inflammatory response is present at the earliest stages of cancer, resulting from small alterations to local tissue architecture. If so, this model may be useful to study the contribution of the inflammatory host response to tumor development and progression. It is well known that an inflammatory environment can drive cancer processes (Coussens and Werb, 2002), and in this case, it may stimulate mutations in addition to the APC mutation that are needed for tumor development. More work needs to be done to determine whether the observed plasma protein elevations indeed represent a host response to incipient cancer or rather a general response to the mutation. The analysis of the time of onset of the inflammatory response, using serially collected samples, would help answer that question. Similar studies could be used to screen for the onset of tumor-specific markers. The low-volume methods described here make such studies possible, since small volumes would be collected from serial, non-terminal bleeds. Such applications

Table 3 – Rank-correlations (Spearman's rho) between protein concentrations and the indicated parameters

Protein	Correlation in mutants		Correlation in wildtypes
	To number of tumors	To age	To age
CRP	−0.030 (0.8)	−0.21 (0.2)	−0.050 (0.8)
IL-12	**−0.30 (0.02)**	−0.19 (0.2)	0.34 (0.09)
Haptoglobin	0.33 (0.05)	**0.43 (0.002)**	0.11 (0.6)
Hemopexin	**0.47 (0.0005)**	**0.41 (0.006)**	−0.12 (0.5)
Plasminogen	0.050 (0.8)	0.010 (0.9)	0.17 (0.4)
IL-2	−0.29 (0.06)	−0.25 (0.1)	**−0.51 (0.003)**
IL-10	−0.19 (0.3)	0.070 (0.7)	0.26 (0.2)
Alpha-1 -antitrypsin	−0.010 (1)	0.17 (0.2)	**−0.38 (0.04)**
VEGF	0.020 (0.9)	0.18 (0.3)	0.19 (0.4)
Clusterin	0.13 (0.4)	−0.060 (0.7)	−0.090 (0.7)
IL-6	**0.52 (0.0002)**	**0.66 (6×10^{-10})**	0.20 (0.4)
IL-1alpha	−0.19 (0.3)	−0.22 (0.18)	0.17 (0.4)

The p-value of the correlation is shown in parentheses. Values with $p \leq 0.05$ are in bold type.

highlight another advantage of using mouse models for cancer research studies, since analagous studies are difficult with human subjects.

CRP is not as strongly induced in mouse as in human in response to inflammatory situations (Ku and Mortensen, 1993). The average CRP elevation in this study was 5.16-fold, compared to an average 13.6-fold elevation found in a recent study of sera from human lung cancer patients (Gao et al., 2005). Although the level of CRP induction is not as high as in humans, the consistency of the elevation in mice is very high, showing a 90% sensitivity for cancer detection at an 80% specificity. This consistency may indicate a central role for CRP in mouse inflammatory processes or may reflect the genetic and environmental similarity of the mice. Other proteins, such as alpha-1-antitrypsin and VEGF, had highly variable levels in the mutant mice despite the similarities between the mice. Those proteins also are highly variable in human cancer patients (Gao et al., 2005). They were not highly important for the classification of the samples using DLDA, probably because of their high variability.

The elevation of IL-6, haptoglobin, and hemopexin after the mice show about 30–40 tumors could indicate that these molecules are important for regulating a heightened stress response. The increased levels also could be due to the malabsorption secondary to the large tumor burden or the low level intestinal bleeding known to occur in these mice. Given that IL-6 has been associated with cachexia (Barton and Murphy, 2001), this model might provide a useful resource for studying late-stage cancer processes.

The perfect discrimination of the mutant mice from the wildtype mice using a small number of marker proteins probably stems from the genetic and environmental similarity of the mice and their tumors. That level of discrimination would likely not be possible for human cancer using these proteins. The sensitive and specific detection of cancer-related abnormalities seen here supports the use of mouse models for new marker discovery. We had no success using anti-human antibodies to measure mouse proteins, but it would be valuable to have antibodies that reacted equally well with the human and mouse sequences, so that expression levels could be easily compared between human cancers and mouse models.

In summary, this work demonstrates a practical new approach for profiling multiple proteins in mouse models of cancer, and the application of this method revealed the presence of a consistent inflammatory response even at the earliest cancer stages. This method could be used to further study and identify inflammatory mediators of cancer development and progression. Another logical application of this method would be to validate candidate biomarkers identified by mass-spectrometry studies on mouse models of cancer. Low-volume immunoassay methods also could be useful in other cases where limited sample is available, such as certain types of clinical specimens or rare cell populations. The methods developed here provide a method for the routine application of antibody-based methods to such studies.

4. Experimental procedures

4.1. *Animal husbandry*

Mice were purchased from the Jackson Laboratories. Heterozygous APC^{Min} or APC Δ580 mice on the C57bl/6 (B6)

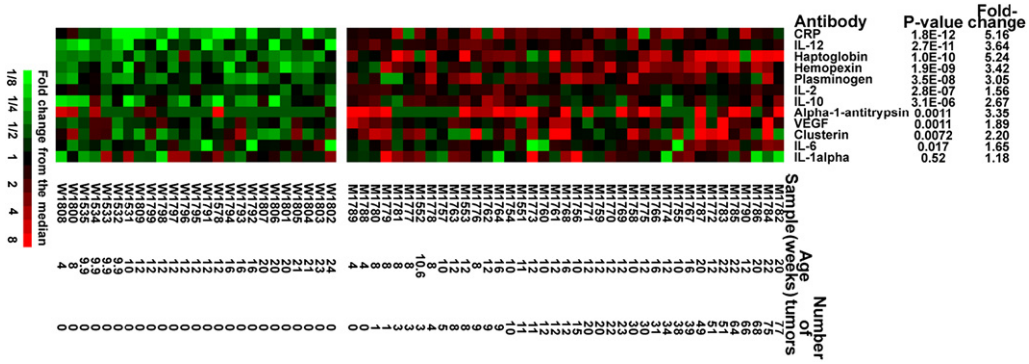

Figure 4 – Protein expression profiles. The samples are arranged in order of increasing tumor burden for the mutant mice. The assays are arranged in order of increasing p-values from two-sample T-tests comparing the mutant and wild-type mice. Each colored square indicates the fold differences from the median of all samples for a particular analyte, according to the color bar at left.

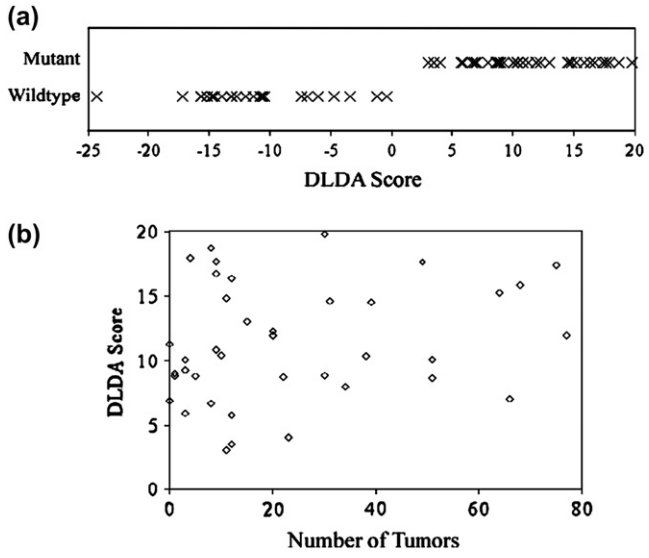

Figure 5 – Sample classification. (a) Scores from leave-one-out cross-validation of diagonal linear discriminant analysis (DLDA) classifiers, using seven proteins. (b) The DLDA score of each sample is plotted with respect to the number of tumors in the given sample. The Spearman's rho correlation between the two parameters was 0.19 ($p = 0.20$).

background were mated with wild-type B6 mice. The APC^{Min} mice contain a nonsense mutation at codon 850, and the APC Δ580 mice were created by a targeted deletion of exon 14 of the APC gene resulting in a nonsense mutation at codon 580. The resulting offspring were screened by PCR of tail DNA using standard methods. Heterozygous APC^{Min} or APC Δ580 mice were used for the studies. Wild-type age- and sex-matched littermates were used as controls.

4.2. *Plasma collection and tumor quantification*

A lethal coma was induced by intraperitoneal injection of avertin, and blood was removed by cardiac puncture. Blood was centrifuged at 1500 rpm for 10 min at 4 °C in EDTA-coated tubes. Plasma supernatants were removed and stored at −80 °C. The samples were thawed, sub-aliquoted, and re-frozen once prior to analysis. The small and large bowel were removed and opened longitudinally, and the number of tumors was counted using a dissecting microscope.

4.3. *Antibodies*

Antibodies were purchased from various sources (Table 1). The antibodies were prepared at concentrations of 0.5 mg/ml in 10.1 mmol/l Na_2HPO_4, 1.8 mmol/l KH_2PO_4, 137 mmol/l NaCl, and 2.7 mmol/l KCl (pH 7.5; 1× PBS) containing 0.02% NaN_3. The integrity of each antibody was confirmed by reducing and non-reducing gel electrophoresis.

4.4. *Microarray preparation*

A piezoelectric non-contact printer (Biochip Arrayer, PerkinElmer Life Sciences) spotted approximately 350 pl of each antibody solution onto the surfaces of ultra-thin, nitrocellulose-coated microscope slides (PATH slides, GenTel Biosurfaces). Forty-eight or 192 identical arrays were printed on each slide, spaced by 4.5 mm or 2.25 mm, respectively. Each array consisted of 6–36 antibodies and control proteins spotted in triplicate. A wax border was imprinted around each of the arrays to define hydrophobic boundaries, using a custom-built device.

4.5. *Sandwich assays*

Samples (either plasma or purified proteins) were diluted into 1× phosphate-buffered saline (PBS) buffer containing 0.01% Brij, and 0.01% Tween-20. The microarray slides were washed in phosphate-buffered saline containing 0.5% Tween-20 (PBST0.5) three times for 3 min each to remove unbound antibodies and clean the surface, and they were placed in a blocking solution of PBST0.5 containing 1% BSA at room temperature for 1 h. The slides were washed in three baths of PBST0.1 and spun dry. Either 6 or 1.5 μl of sample (and same volumes for subsequent incubations) were applied to each array and incubated at room temperature for 1 h. Six microliters were applied to the larger arrays (on slides with 48 arrays), and 1.5 μl were applied to the smaller arrays (on slides with 192 arrays). After washing and spin-drying the slides as above, 1 μl/ml detection antibody in PBST0.1 containing 0.1% BSA was applied to each array and incubated at room temperature for 1 h. The slides were washed and spun dry, and 1 μl/ml streptavidin-phycoerythrin (Roche Applied Science) in PBST0.1 was applied to each array and incubated at room temperature for 1 h. The slides were given a final wash and dry, and fluorescence emission was detected at 570 nm using a microarray scanner (ScanArray Lite, PerkinElmer Life Sciences). All arrays assaying the same protein were scanned in one sitting at a single laser power and detector gain setting.

The software program GenePix Pro 5.0 (Molecular Devices) was used to quantify the image data. Median local backgrounds were subtracted from the median intensity of each spot, and data from replicate spots were averaged (geometric mean). The data were not normalized. The reference curves were created by fitting the fluorescence values using a four-parameter, non-linear regression curve using the Origin software program. The protein concentrations in the samples were calculated according to the resulting equations.

4.6. *Statistical analysis*

The data were log-transformed after adding one-tenth of the mean for each analyte. We compared mutant to wild-type mouse samples using two-sample *T*-tests, and estimated fold-changes based on the means of the log-transformed data. The original and log-transformed data are available in the supplementary information (Supplementary Table 1). We used diagonal linear discriminant analysis (DLDA) to give classification scores to each sample (Dudoit et al., 2002). We used leave-one-out-cross-validation of the classifiers, in which each sample is removed from the data set, one sample at a time, the best assays (judged by *T*-tests) and their weights in the DLDA discriminant function then determined based

only on the remaining samples, and the resulting score computed for the left out sample.

Acknowledgements

We gratefully acknowledge support of this work from the SAIC/NCI (contract 23Xs110A to the Eastern Consortium for Proteomics Analyses of Mouse Models of Human Cancers, subcontract F012596, B.B.H. and S.F.); the Michigan Technology Tri-Corridor (Proteomics Alliance for Cancer Research, grant GR-687, B.B.H., S.F. and R.K.); the NIDDK (1K08DK078033-01, K.H.); the American Gastroenterological Association (Research Scholar Award, K.H.); and the Van Andel Research Institute (B.B.H. and S.F.).

Appendix A. Supplementary data

Supplementary data associated with this article can be found, in the online version, at doi:10.1016/j.molonc.2007.06.001.

REFERENCES

Barton, B.E., Murphy, T.F., 2001. Cancer cachexia is mediated in part by the induction of IL-6-like cytokines from the spleen. Cytokine 16, 251–257.

Coussens, L.M., Werb, Z., 2002. Inflammation and cancer. Nature 420, 860–867.

Dudoit, S., Fridlyand, J., Speed, T.P., 2002. Comparison of discrimination methods for the classification of tumors using gene expression data. J. Am. Stat. Assoc. 97, 77–87.

Etzioni, R., Urban, N., Ramsey, S., McIntosh, M., Schwartz, S., Reid, B., Radich, J., Anderson, G., Hartwell, L., 2003. The case for early detection. Nat. Rev. Cancer 3, 243–252.

Gao, W.M., Kuick, R., Orchekowski, R.P., Misek, D.E., Qiu, J., Greenberg, A.K., Rom, W.N., Brenner, D.E., Omenn, G.S., Haab, B.B., Hanash, S.M., 2005. Distinctive serum protein profiles involving abundant proteins in lung cancer patients based upon antibody microarray analysis. BMC Cancer 5, 110.

Geierstanger, B.H., Saviranta, P., Brinker, A., 2006. Antibody microarrays using resonance light-scattering particles for detection. Methods Mol. Biol. 328, 31–50.

Haab, B.B., 2006. Applications of antibody array platforms. Curr. Opin. Biotechnol 17, 415–421.

Haab, B.B., Dunham, M.J., Brown, P.O., 2001. Protein microarrays for highly parallel detection and quantitation of specific proteins and antibodies in complex solutions. Genome Biol. 2, 1–13.

Honda, N., Lindberg, U., Andersson, P., Hoffmann, S., Takei, H., 2005. Simultaneous multiple immunoassays in a compact disc-shaped microfluidic device based on centrifugal force. Clin. Chem. 51, 1955–1961.

Huang, R.-P., Huang, R., Fan, Y., Lin, Y., 2001. Simultaneous detection of multiple cytokines from conditioned media and patient's sera by an antibody-based protein array system. Anal. Biochem 294, 55–62.

Hung, K.E., Kho, A.T., Sarracino, D., Richard, L.G., Krastins, B., Forrester, S., Haab, B.B., Kohane, I.S., Kucherlapati, R., 2006. Mass spectrometry-based study of the plasma proteome in a mouse intestinal tumor model. J. Proteome Res. 5, 1866–1878.

Kingsmore, S.F., 2006. Multiplexed protein measurement: technologies and applications of protein and antibody arrays. Nat. Rev. Drug Discov 5, 310–320.

Kinzler, K.W., Vogelstein, B., 1996. Lessons from hereditary colorectal cancer. Cell 87, 159–170.

Ku, N.O., Mortensen, R.F., 1993. The mouse C-reactive protein (CRP) gene is expressed in response to IL-1 but not IL-6. Cytokine 5, 319–326.

Kuick, R., Misek, D.E., Monsma, D.J., Webb, C.P., Wang, H., Peterson, K.J., Pisano, M., Omenn, G.S., Hanash, S.M., 2007. Discovery of cancer biomarkers through the use of mouse models. Cancer Lett. 249, 40–48.

Lai, S., Wang, S., Luo, J., Lee, L.J., Yang, S.T., Madou, M.J., 2004. Design of a compact disk-like microfluidic platform for enzyme-linked immunosorbent assay. Anal. Chem. 76, 1832–1837.

Li, Y., Reichert, W.M., 2003. Adapting cDNA microarray format to cytokine detection protein arrays. Langmuir 19, 1557–1566.

Perlee, L., Christiansen, J., Dondero, R., Grimwade, B., Lejnine, S., Mullenix, M., Shao, W., Sorette, M., Tchernev, V., Patel, D., Kingsmore, S., 2004. Development and standardization of multiplexed antibody microarrays for use in quantitative proteomics. Proteome Sci. 2, 9.

Schweitzer, B., Roberts, S., Grimwade, B., Shao, W., Wang, M., Fu, Q., Shu, Q., Laroche, I., Zhou, Z., Tchernev, V.T., Christiansen, J., Velleca, M., Kingsmore, S.F., 2002. Multiplexed protein profiling on microarrays by rolling-circle amplification. Nat. Biotechnol 20, 359–365.

Shaw, A.T., Kirsch, D.G., Jacks, T., 2005. Future of early detection of lung cancer: the role of mouse models. Clin. Cancer Res. 11, 4999s–5003s.

Sreekumar, A., Nyati, M.K., Varambally, S., Barrette, T.R., Ghosh, D., Lawrence, T.S., Chinnaiyan, A.M., 2001. Profiling of cancer cells using protein microarrays: discovery of novel radiation-regulated proteins. Cancer Res. 61, 7585–7593.

Su, L.K., Kinzler, K.W., Vogelstein, B., Preisinger, A.C., Moser, A.R., Luongo, C., Gould, K.A., Dove, W.F., 1992. Multiple intestinal neoplasia caused by a mutation in the murine homolog of the APC gene. Science 256, 668–670.

Vignali, D.A., 2000. Multiplexed particle-based flow cytometric assays. J. Immunol. Methods 243, 243–255.

Wingren, C., Borrebaeck, C.A., 2006. Antibody microarrays: current status and key technological advances. Omics 10, 411–427.

Wingren, C., Steinhauer, C., Ingvarsson, J., Persson, E., Larsson, K., Borrebaeck, C.A., 2005. Microarrays based on affinity-tagged single-chain Fv antibodies: sensitive detection of analyte in complex proteomes. Proteomics 5, 1281–1291.